EPJ D

www.epj.org

Atomic, Molecular, Optical and Plasma Physics

Eur. Phys. J. D **52**, 107–110 (2009) DOI: 10.1140/epjd/e2009-00065-1

Pinning of size-selected Co clusters on highly ordered pyrolytic graphite

S. Vučković, J. Samela, K. Nordlund and V.N. Popok

EDP SCIENCES

Società Italiana di Fisica

Springer

Eur. Phys. J. D **52**, 107–110 (2009)
DOI: 10.1140/epjd/e2009-00065-1

THE EUROPEAN PHYSICAL JOURNAL D

Regular Article

Pinning of size-selected Co clusters on highly ordered pyrolytic graphite

S. Vučković[1,a], J. Samela[2], K. Nordlund[2], and V.N. Popok[1]

[1] Department of Physics, University of Gothenburg, 412 96 Gothenburg, Sweden
[2] Department of Physics, University of Helsinki, 00014 Espoo, Finland

Received 19 September 2008
Published online 6 March 2009 –

Abstract. Deposition and implantation of size-selected $Co^+_{50\pm5}$ cluster ions on/in highly ordered pyrolytic graphite (HOPG) have been performed. Cobalt clusters were produced by laser ablation using the second harmonic (532 nm) of a Nd:YAG laser. They were deposited/implanted with energies of 250–4850 eV/cluster and examined using scanning tunneling microscopy (STM). For the highest energies the clusters created craters and wells with residual clusters at the bottom of the wells. Decrease of the impact energy led to formation of bumps which consist of damaged graphite areas mixed with fragmented cobalt clusters. Further decrease of the impact energy to 250–450 eV/cluster probably corresponds to the so-called pinning regime, when the impacting cluster creates defects in the surface layer and becomes bound to them. The transition from implantation to pinning with a decrease of impact energy was confirmed by etching experiments showing the depth of the damage introduced by the cluster collisions with HOPG.

PACS. 61.46.Bc Structure of clusters – 61.80.Jh Ion radiation effects – 68.37.Ef Scanning tunneling microscopy – 79.20.Ap Theory of impact phenomena; numerical simulation

1 Introduction

Nowadays, atomic and molecular clusters with sizes on the nm-scale made of different species are the subjects of intensive study. For the last decade, there has been a growing interest in how the size reduction affects electronic, magnetic, optical and some other properties of nano-objects. These properties can be controlled to a certain extent to meet technological requirements for applications in nanotechnology. Clusters have been extensively studied in the gas phase but for most technological applications they need to be deposited on a surface or embedded in the bulk. Thus, interaction of a cluster with the substrate needs to be understood for the development of useful cluster-based technologies. Cluster ion beam interaction is a novel method for surface modification on the nano-scale, such as surface smoothing, sputtering and shallow implantation [1–3]. It is also an efficient tool for building of nanostructures [2,4]. Here, the control of the cluster size and its kinetic (impact) energy becomes one of the main advantages of the cluster beam technique, compared to other methods of nanoparticle formation [5,6]. For some applications the control of the cluster structure and size on a surface is needed. This requires suppressing a possible diffusion of the deposited clusters on the surface that can be achieved by several methods, for instance, by cooling to low temperatures or by preparing surface patterns that favour cluster ordering [7,8]. Another possibility is to vary the cluster kinetic energy approaching the so-called pinning regime when the defects created in the surface layer by cluster impact serve as efficient binding centres preventing cluster diffusion [9].

In this paper we present the results of a STM study of HOPG surfaces after the impact of size-selected Co clusters having different kinetic energies, thus, providing evidence for change of the cluster-surface interaction mechanism from implantation to deposition. The experimental results are compared with the preliminary molecular dynamics (MD) simulations.

2 Experimental

Cobalt clusters were produced by the laser vaporisation method using a laser ablation cluster source (LACS). The second harmonic (532 nm) of a Nd:YAG laser was utilised. More details on the LACS construction and parameters can be found elsewhere [10]. A typical mass spectrum of the obtained Co^+_n clusters is presented in Figure 1. Mean cluster sizes are estimated using the spherical cluster approximation

$$D = 2R_{WS}(n/f)^{1/3} \quad (1)$$

[a] e-mail: sasa.vuckovic@physics.gu.se

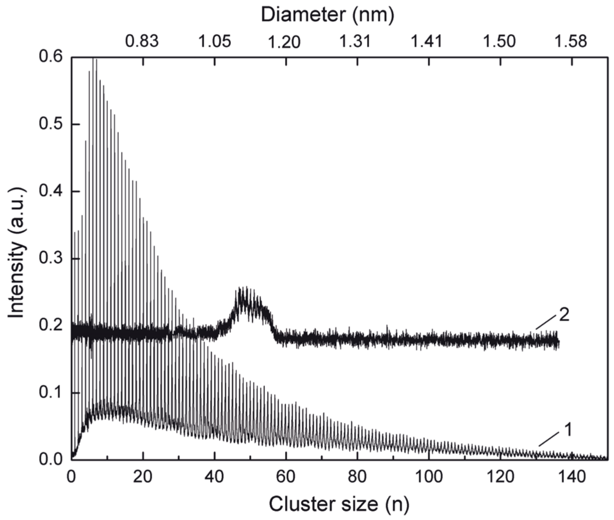

Fig. 1. Mass-spectra of Co_n^+ cluster ions before (1) and after (2) size selection.

where D is the diameter, R_{WS} is the Wigner-Seitz radius for Co and f is the packing factor assumed to be 0.74. The source was connected to a cluster implantation and deposition apparatus (see for details [11,12]) which gives the possibility of size selecting the clusters, and control of their kinetic energy.

For the present experiments clusters of cobalt with $n = 50 \pm 5$ were chosen (Fig. 1). They were deposited/implanted on/in a freshly cleaved surface of HOPG in vacuum of (2–3) $\times 10^{-9}$ torr. Kinetic energies varied from 250 to 4850 eV/cluster that gives mean energy from 5 to 97 eV/atom. After the cluster impact the samples were studied by STM (Ntegra-Aura, NT-MDT) in the constant current mode with a bias of 0.1 V using PtIr tips. After the initial STM study the samples were annealed at 600 °C for 3 min in a furnace in ambient atmosphere. This procedure provides effective etching of the graphite areas damaged on the cluster impact due to their oxidation [13]. The etched samples were studied again by STM under the same conditions.

The simulations were carried out using classical MD. An improved Tersoff potential [14] was used to describe the graphite interactions, including the interlayer interaction. The Co–Co interactions were modelled applying the embedded atom method [15]. A Morse potential was used to describe the C–Co interaction so that the equilibrium distance was 2.0 Å and the corresponding binding energy –1.5 eV. A rectangular simulation box (20 × 20 × 20 nm) was chosen to be large enough to include the zone of oscillating graphite layers around the impact point and to prevent boundary effects from distorting the cascades. The ambient temperature in the simulation was 300 K. The time of simulation was limited to 2 ps for the preliminary study. Although, the oscillations of the lattice are not completely finished, the radiation cascade is already developed and that allows the depth of the damage introduced by the cluster impact to be estimated.

3 Results and discussion

Clusters of $Co_{50\pm5}$ were deposited with different energies on HOPG and the corresponding STM images can be seen in Figure 2. Figure 2a shows the HOPG surface bombarded by the clusters with the highest chosen energy (97 ± 10 eV/atom). Formation of radiation damaged areas which are about 2.0–2.5 nm in diameter can be seen. The structure of these areas looks like partly filled craters or wells. In some cases a centrally positioned bump can be seen. This cluster energy lies in the high energetic regime where the kinetic energy per atom is much higher than the binding energy of atoms in the cluster, which is on the order of a few eV according to theoretical calculations [16–18]. The clusters fragment during the impact and come to rest in the open well that has been produced due to the energetic impact. This scenario of energetic impact of various cluster species with graphite was theoretically suggested elsewhere [9,19,20].

It is known that oxidative etching of untreated graphite at 650 °C can lead to formation of 1 monolayer (ML) deep pits due to presence of defects in the very top layer [21]. These pits are typically circular or hexagonal in shape. The diameter depends on the etching time. It was shown elsewhere that monomer or cluster ion implantation followed by etching leads to the formation of deeper pits [13]. The depth of the pits depends on the depth of the radiation damage cascades developed by the projectiles. Thus, the etching removes only the damaged graphite and it should not typically attack the graphite planes below the damaged volume. Hence, one can estimate the radiation damage depth from the etching experiments.

Figure 2b shows the HOPG surface bombarded by 4.85 keV Co clusters (97 eV/atom) after the subsequent etching. Systematic analysis shows some minor number of pits which are 1–2 ML deep. Their shape is close to circular. These pits can be disregarded because they are most probably related to some natural defects in the top layers of HOPG. The majority of pits are 3–5 ML deep and they have a worm-like shape (Fig. 2b). The length of these channels can reach some tens of nm. The depth corresponds very well to preliminary MD simulation results of 5 keV implantation of Co_{50} clusters into graphite showing damage for up to 5–6 ML (Fig. 3a). However, to our knowledge the worm-like shape of the pits is observed for the first time for the case of cluster implantation. These channels most probably represent the paths of randomly moving residual Co atoms and clusters located at the bottom of the craters after impact. High temperature increases diffusive mobility of the cobalt clusters and they catalyse the reaction of atmospheric oxygen with carbon thus favouring the formation of random in shape planar surface channels. Similar effects were reported elsewhere on deposition of various chemical substances on graphite surfaces followed by etching [21].

Decreasing the kinetic energy to 1500 eV/cluster (mean energy of 30 ± 3 eV/atom) leads to conversion of the impact defects from the crater or well-like structures towards small bumps, see Figure 2c. These structures have a mean diameter of ∼3 nm and a height of ∼0.45 nm.

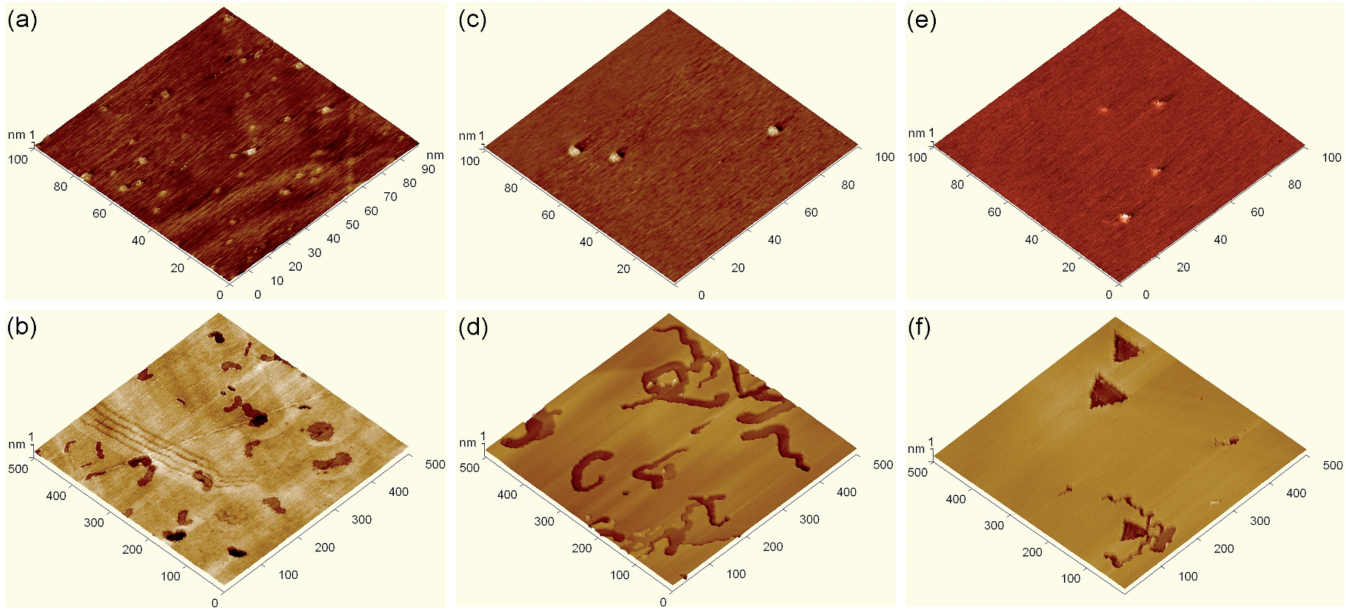

Fig. 2. (Color online) STM images of HOPG after cluster impact with energies of (a) 97, (c) 30 and (d) 9 eV/atom. Images (b), (d) and (f) show the corresponding samples after etching.

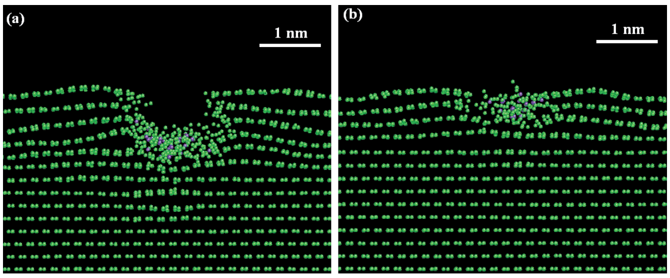

Fig. 3. (Color online) MD simulation snapshots (after 2 ps) of Co_{50} cluster impact on graphite with energies of (a) 5 keV/cluster (100 eV/atom) and (b) 1.5 keV/cluster (30 eV/atom).

The impact energy is still high enough to break the clusters on impact but too low to form craters. Those bumps are most probably formed by intermixture of the cobalt atoms from the broken clusters and carbon atoms that are displaced on the cluster impact. The etched sample (Fig. 2d) shows longer worm-like channels compared to the previous sample. Up to 2 ML have been etched away showing that this energy is not enough to create deep damage. This result agrees very well with the MD simulation (Fig. 3b) showing no crater formation and the damage of 2–3 ML of graphite. The longer channels are probably related to the fact that the clusters are less fragmented and located in very shallow regions that favours their higher mobility and catalytic activity.

Further decrease of the kinetic energy down to 450–250 eV/cluster (mean energy of 9–5 eV/atom) leads to formation of surface bumps that are very similar for all these above energies (Fig. 2e). The bumps have a diameter of 1.4–1.5 nm and a height of 0.3 nm. It was suggested elsewhere that pinning of clusters occurs when the cluster provides enough energy E_T to produce a carbon atom displacement in the substrate [9]. The developed model yields the threshold pinning energy

$$E_{pin} = nM_e \frac{E_T}{4M_C} \qquad (2)$$

where n is the number of atoms in the cluster, M_e is the atomic mass of the chemical element of the cluster, and M_C is the atomic mass of the target atoms. This model was developed for Ag_n clusters and HOPG and later was proved for other clusters species [22,23]. In the model one should consider that E_T is not a constant. Experimentally obtained and theoretically predicted values for the formation of vacancies or interstitials in graphite vary between 4.75 and 7.0 eV [24]. Taking into account these numbers equation (2) will yield a pinning window of ca. 5.8–8.6 eV/atom for Co_{50} clusters. This predicted interval is in good agreement with the observation of very similar bumps on the impact of clusters with mean energies of 5, 6, 7 and 9 eV/atom. One should also remember that the clusters used in the experiment varied in size between 45–55 atoms that will give about 10% deviation from the mean energy values. From the size of the bumps (diameters are about 5 times larger than heights) one can conclude that the clusters are flattened on impact. However, some enlargement in diameters can also be expected from the STM tip convolution. The suggested pinning "window" of 5–9 eV/atom for the cobalt clusters is in agreement with the mean pinning energy of 5.7 eV/atom suggested elsewhere for Ni clusters [22]. Since Co and Ni have very close atomic masses this fact supports the validity of equation (2).

Heating of the sample implanted by clusters with energy of 450 eV/cluster (9 eV/atom, Fig. 2f) at 600 °C leads to the formation of circular or sometimes triangular 1–2 ML deep pits, which are probably related to natural point defects, and 1–2 ML deep worm-like channels originated by catalytic-activated etching of the graphite surface by moving Co clusters.

4 Conclusion

Size-selected $Co_{50\pm5}$ clusters were deposited on HOPG with different kinetic energies. Clusters with mean impact energy of 4.85 keV/cluster (97 eV/atom) created radiation damaged areas with a diameter of 2.0–2.5 nm representing partly filled craters. Oxidative etching of the sample allowed estimating the depth of the radiation cascade developed on the cluster impact which is found to be up to 5 ML. However, in contrast to implantation of inert gas or noble metal clusters, the residual cobalt clusters located at the bottom of craters catalysed intensive oxidative etching in planar directions that led to the formation of random in shape (worm-like) channels.

Decrease of the mean cluster kinetic energy to 1.5 keV/cluster (30 eV/atom) led to conversion of the impact defects from craters to small bumps. These structures are probably formed by intermixture of the fragmented cobalt clusters and carbon atoms. Worm-like channels with depth of 2 ML were also observed after the etching. Since the clusters are less fragmented compared to higher energy implantation and they are located almost on the surface, their catalytic activity is higher and causes much longer etched channels.

Further decrease of the kinetic energy to 250–450 eV/cluster (5–9 eV/atom) led to formation of surface bumps with diameter of ∼1.4 nm and height of 0.3 nm. Etching of these samples revealed the formation of worm-like channels with 1–2 removed ML of graphite. Comparison of the experimental results with the pinning model developed elsewhere [9,22] suggests that the kinetic energy interval between 5 and 9 eV/atom for Co_{50} clusters can correspond to their pinning on the HOPG surface and the observed bumps are clusters that have been flattened on impact.

The financial support of the Swedish Research Council under the project No. 621-2005-6272 is acknowledged. Two of the authors (S.V. and V.N.P.) are also grateful for the support of the Nanoparticle Platform at the Science Faculty of the University of Gothenburg.

References

1. I. Yamada, N. Toyoda, Nucl. Instrum. Meth. B **241**, 589 (2005)
2. W. Habrich, in *Metal Clusters at Surfaces*, edited by K.H. Maiwess-Broer (Springer, Berlin, 2000), p. 107
3. V.N. Popok, E.E.B. Campbell, Rev. Adv. Mater. Sci. **11**, 19 (2006)
4. K. Wegner, P. Piseri, H. Vahedi Tafreshi, P. Milani, J. Phys. D: Appl. Phys. **39**, R439 (2006)
5. J.P. Wilcoxon, J.E. Martin, P. Provencio, J. Chem. Phys. **115**, 998 (2001)
6. B. Bennewitz, J.N. Crain, A. Kirakosian, J.-L. Lin, J.L. McChesney, D.Y. Petrovykh, F.J. Himpsel, Nanotechnology **13**, 49 (2002)
7. L. Bardotti, B. Prevel, P. Jensen, M. Treilleux, P. Melinon, A. Perez, J. Gierak, G. Faini, D. Mailly, Appl. Surf. Sci. **191**, 205 (2002)
8. U. Queitsch, E. Mohn, F. Scaffel, L. Schultz, B. Rellinghaus, A. Bluher, M. Mertig, Appl. Phys. Lett. **90**, 113114 (2007)
9. S.J. Carrol, P.D. Nellist, R.E. Palmer, S. Hobday, R. Smith, Phys. Rev. Lett. **84**, 2654 (2000)
10. S. Vučković, V.N. Popok, Rev. Sci. Instrum. **79**, 073303 (2008)
11. V.N. Popok, S.V. Prasalovich, M. Samuelsson, E.E.B. Campbell, Rev. Sci. Instrum. **73**, 4283 (2002)
12. V.N. Popok, S.V. Prasalovich, E.E.B. Campbell, Nucl. Instrum. Meth. B **207**, 145 (2003)
13. G. Bräuchle, S. Richard-Scheider, D. Illig, R.D. Beck, H. Schreiber, M.M. Kappes, Nucl. Instrum. Meth. B **112**, 105 (1996)
14. K. Nordlund, J. Keinonen, T. Mattila, Phys. Rev. Lett. **77**, 699 (1996)
15. K.W. Jacobsen, J.K. Norskov, M.J. Puska, Phys. Rev. B **35**, 7423 (1987)
16. M. Castro, C. Jamorski, D.R. Salahub, Chem. Phys. Lett. **271**, 133 (1997)
17. Q.-M. Ma, Z. Xie, J. Wang, Y. Liu, Y.-Ch. Li, Phys. Lett. A **358**, 289 (2006)
18. R. Guirado-Lopez, F. Aguilera-Granja, J.M. Montejano-Carrizales, Phys. Rev. B **65**, 045420 (2002)
19. J. Samela, K. Nordlund, J. Keinonen, V.N. Popok, E.E.B. Campbell, Eur. Phys. J. D **43**, 181 (2007)
20. C. Anders, H.M. Urbasek, Nucl. Instrum. Meth. **228**, 57 (2005)
21. H. Chang, A.J. Bard, J. Am. Chem. Soc. **113**, 5588 (1991)
22. M. Di Vece, S. Palomba, R.E. Palmer, Phys. Rev. B **72**, 073407 (2005)
23. S. Gibilisco, M. Di Vece, S. Palomba, G. Faraci, R.E. Palmer, J. Chem. Phys. **125**, 084704 (2006)
24. R. Smith, C. Nock, S.D. Kenny, J.J. Belbruno, M. Di Vece, S. Palomba, R.E. Palmer, Phys. Rev. B **73**, 125429 (2006)